Sulfonate anionic small molecule as a cathode interfacial material for highly efficient polymer solar cells†

Changjian Song,[ab] Xiaohui Liu,[b] Xiaodong Li,[b] Wenjun Zhang,*[b] Yueling Bai[a] and Junfeng Fang*[b]

The cathode interlayer is essential to bulk heterojunction polymer solar cells (PSCs). As we all know, most of the organic interfacial materials are amino derivatives, including neutral amine derivatives and ammonium derivatives. Herein, a non-amino small molecule, **TBT-a**, with sulfonate anionic pendants was synthesized and interface modification was investigated. The PSC with **TBT-a** as the cathode interlayer exhibited a high power conversion efficiency of 8.68%. We found that the **TBT-a** interlayer simultaneously enhanced all the device parameters, probably by inducing an effective interface dipole, altering the optical distribution, and enhancing the electron mobility. These results indicated that sulfonate interfacial materials could play a similar role as amine-based interfacial materials in interface modification.

Introduction

Bulk heterojunction (BHJ) polymer solar cells (PSCs) have attracted an enormous amount of attention during recent decades due to their potential applications in flexible, low-cost, and large-area devices through solution processing.[1–5] A sandwich structure is the typical architecture for PSCs, where the photoactive materials are sandwiched between the anode and cathode. The power conversion efficiencies (PCEs) of PSC devices have been significantly improved, with the appearance of new photo-absorption materials and interfacial materials, at the same time, with the optimization of active-layer morphology and fabrication processes.[6–14] Although the photoactive materials play an essential role in light absorption, the interfacial materials also have a crucial function in carrier collection and extraction.[11,13,15–17] The insertion of interlayer can significantly affect the parameters due to its abilities to tune the energy level alignment, improve charge transport at interface, promote the adhesion between electrode and active layer and enhance light-trapping by optical spacer effect.[18–21] Hence, the interfacial modification layers inserted between electrodes and active layer are necessary.

Owing to the good solution-processing ability and interface modification, various alcohol/water-soluble organic materials have been developed as cathode interfacial materials for PSCs.[8,22–28] For these interfacial materials, they usually possess a highly polar chain, which can form an efficient interfacial dipole and facilitate electron collection and extraction, together with a conjugated or non-conjugated unit. For example, a famous interfacial material poly[(9,9-bis(3′-(*N*,*N*-dimethylamino)propyl)-2,7-fluorene)-*alt*-2,7-(9,9-dioctylfluorene)] (PFN) was introduced to PSCs by Cao group, and a high PCE of 9.2% was obtained with simultaneous increase in the short-circuit current (J_{sc}), open circuit voltage (V_{oc}), and fill factor (FF).[11] Although the alcohol/water-soluble organic interfacial materials have been widely studied, the structural variety is poor. Most of the interfacial materials derived from amino, including neutral amine derivatives and ammonium derivatives.[13,19,27–33] Cathode interfacial materials without amine or ammonium group are limitedly reported and efficiency of the PSCs based on them need to be further improved.[26,34,35]

Anionic conjugated polymers with sulfonate pendant have been used in PSCs as anode interfacial materials.[35–37] However, as we known, the ammonium zwitterions have been widely used as cathode interfacial materials, which also possess sulfonate anion.[19,38] Spontaneously, it is doubt that whether organic materials with separate sulfonate anion can work out as cathode interfacial materials. Our former researches have certified that alcohol/water-soluble small molecules are also preeminent candidates to cathode interfacial materials. Compared to conjugated polymers, they are synthesized simply without complex C–C coupling and polymerization reactions and easy to purify. What's more, they are mono disperse in nature with specified chemical structure, and the small molecules are synthetized with good reproducibility.

Herein, we designed and synthesized a small molecule **TBT-a** with sulfonate anionic pendants. Fortunately, this sulfonate

[a]*Department of Chemistry, College of Science, Shanghai University, Shanghai 200444, China*

[b]*Ningbo Institute of Materials Technology and Engineering, Chinese Academy of Sciences, Ningbo 315201, China. E-mail: zhangwenjun@nimte.ac.cn; fangjf@nimte.ac.cn*

small molecule exhibited an excellent interfacial ability in PSC cathode. The conventional PSC with **TBT-a** as cathode interlayer exhibited a high PCE as high as 8.68%, which is over 20% enhancement than the device only treated with MeOH. This indicated that not only amino-based molecules were efficient cathode interfacial materials, other molecules such as sulfonate-based molecules could be candidates for cathode interfacial materials of highly efficient PSCs.

Experimental

Measurement and characterization

^{1}H and ^{13}C NMR spectra were collected from a Bruker 400 MHz AVANCE III with tetramethylsilane (TMS) as an internal reference, and deuterated dimethyl sulfoxide as solvent. Mass spectra were recorded on a Finnigan LCQ mass spectrometer. UV-vis absorption measurements were taken on a mapada UV-3300 spectrophotometer. The cyclic voltammetric tests (CV) were carried out on a CHI600D electrochemical workstation with a platinum working electrode of 2 mm diameter and a platinum wire counter electrode at a scan rate of 50 mV s^{-1} against a solution (purged with nitrogen for 15 min) of 0.1 mol L^{-1} tetrahydrofuran solution containing tetrabutyl ammonium hexafluorophosphate (Bu_4NPF_6). The film for electrochemical measurements was coated from its aqueous solution. The electrochemical potential was calibrated against ferrocene/ferrocenium redox couple (Fc/Fc^{+}). Scanning Kelvin probe microscopy (SKPM) measurements were carried out on AFM equipment, using the standard SKPM mode. The tapping-mode AFM images were obtained by using a scanning probe microscope (Dimension3100V). The current density–voltage characteristics of the photovoltaic devices were recorded using a computer-controlled Keithley 2400 source meter under 1 sun, AM 1.5G simulated solar light. The measurement of external quantum efficiency (EQE) was performed using an IQE200TM data acquisition system. The thickness of Al was monitored upon deposition by using a crystal thickness monitor (Sycon). The thickness of solid film was measured by a Veeco profiler (Dektak 150).

Materials

All reagents were purchased from commercial sources and used without further purification except tetrahydrofuran (THF), toluene and 1,4-dioxane, which were purified by distillation from Na–K alloy under dry argon atmosphere. Indium tin oxide (ITO) coated glass substrates were purchased from Shenzhen Nan Bo Group, China. Poly(3,4-ethylenedioxythiophene) : polystyrene sulfonic acid (PEDOT : PSS) (Clevious P VP AI 4083) was purchased from H. C. Stark company. Electron donor material poly[[4,8-bis[(2-ethylhexyl)-oxy]benzo-[1,2-*b*:4,5-*b*′]dithiophene-2,6-diyl][3-fluoro-2-[(2-ethylhexyl)-carbonyl]-thieno-[3,4-*b*]thiophenediyl]] (PTB7) and electron acceptor material [6,6]-phenyl-C_{71}-butyric acid methyl ester ($PC_{71}BM$) were purchased from 1-material Chemscitech and ADS, respectively. 4,7-Bis(5-bromo-4-hexylthiophen-2-yl) benzo[*c*][1,2,5]thiadiazole (**1**) and 4-(4,4,5,5-tetramethyl-1,3,2-dioxaborolan-2-yl)phenol (**2**) were prepared according to the literatures.[39,40]

Device fabrication

The organic bulk heterojunction solar cells studied in our work adopted a conventional device structure consisting of ITO substrate/PEDOT : PSS/PTB7 : $PC_{71}BM$/interlayer/Al. The ITO substrates were successively cleaned by a sonication of 30 min in detergent, deionized water, acetone and isopropyl alcohol before being dried in a nitrogen stream. The cleaned ITO substrates were then treated with UV ozone for 20 min. PEDOT : PSS was spin-coated onto ITO substrates at 4000 rpm for 60 s. Then, the PEDOT : PSS films were roasted on a hot plate for 15 min at 140 °C in the air. After dust on the ITO substrates was removed, they were transferred into the argon-filled glove box for the next processing. The electron donor material PTB7 and electron acceptor material $PC_{71}BM$ were mixed together by weight ratio 10 : 15 (totally 25 mg mL^{-1}) and dissolved in chlorobenzene (CB) at 60 °C for at least 8 h with an addition of small amount of 1,8-diiodoctane (DIO) (CB : DIO = 97 : 3, v/v). Then, the mixed solution was spin-coated on the freshly prepared PEDOT : PSS interlayers at 2000 rpm for 120 s. The thickness of the active layers was about 100 nm. Subsequently, the cathode interlayers were spin-coated on the active layers at 4000 rpm for 60 s from their solutions in methanol and deionized water (MeOH : H_2O = 96 : 4, v/v). The optimized concentration of **TBT-a** solution was established to be 1.0 mg mL^{-1}. The thickness of **TBT-a** was 9.0 nm, which was shown in Fig. S1 and Table S1.† Then, these substrates were transferred into a thermal evaporator. At last, 100 nm of Al cathode was deposited through a shadow mask (defined the active area of the devices 0.06 cm^2) onto the interfacial layer by thermo-evaporation in a vacuum chamber with base pressure 1 × 10^{-6} mbar.

Synthesis and characterization

4,4′-(5,5′-(Benzo[*c*][1,2,5]thiadiazole-4,7-diyl)bis(3-hexylthiophene-5,2-diyl))diphenol (3). Compound **1** (315 mg, 0.60 mmol), compound **2** (396 mg, 1.80 mmol), $Pd(PPh_3)_4$ (14 mg, 0.012 mmol) and K_2CO_3 (829 mg, 6.00 mmol) were added to a 100 mL two-neck round-bottom flask. This flask was evacuated and filled with argon three times. Then, DMF (20 mL) and deionized water (10 mL) were transferred into the flask under nitrogen atmosphere. Subsequently, the mixture was refluxed at 90 °C for 48 h. After reaction quenching, the mixture was poured into 30 mL 5 mmol mL^{-1} HCl aqueous and extracted with ethyl acetate (20 mL × 3) for three times. The solvent was removed by rotary evaporation to afford crude product, which was purified by column chromatographic (petroleum ether : ethyl acetate = 3 : 1) to give 192 mg red solid with a 49% yield. ^{1}H NMR (400 MHz, DMSO-D_6), δ (ppm): 9.72 (s, 2H), 8.03–8.01 (d, J = 8 Hz, 4H), 7.32–7.30 (d, J = 8 Hz, 4H), 6.87–6.85 (d, J = 8 Hz, 4H), 2.65–2.62 (d, J = 8 Hz, 4H), 1.65–1.58 (m, 4H), 1.22–1.21 (m, 12H), 0.83–0.80 (t, J = 8 Hz, 6H). ^{13}C NMR (100 MHz, DMSO-D_6), δ (ppm): 157.72, 151.98, 139.95, 138.52, 135.79, 130.39, 130.11, 125.23, 124.86, 124.81, 116.06, 31.45, 30.72, 29.08, 28.66, 22.55, 14.37, MS, found value $[M + H]^+$ 653.11, calculated value [M + H] 653.23.

Sodium 3,3′-(((5,5′-(benzo[*c*][1,2,5]thiadiazole-4,7-diyl)bis(3-hexylthiophene-5,2-diyl))bis(4,1-phenylene))bis(oxy))bis(propane-1-sulfonate) (TBT-a). To a suspension of NaH (60%, 28 mg, 0.70 mmol) in dry THF (8 mL) was added a solution of compound **3** (208 mg, 0.32 mmol) in dry THF (4 mL). The mixture was stirred at room temperature for 60 min and then 1,3-propanesultone (210 mg, 1.72 mmol) was added. Subsequently, the reaction mixture was refluxed for 24 h. After the reaction was completed, the solvent was removed by rotary evaporation. Subsequently, crude product was redissolved in deionized water. Then the solution was added dropwise into alcohol solution, which was stirred, at the same time, the pure product precipitated from alcohol solution. At last, 60 mg of red solid (**TBT-a**) was collected by filtration with a 20% yield. ^{1}H NMR (400 MHz, DMSO-D_6), δ (ppm): 8.07–8.06 (d, J = 4 Hz, 4H), 7.42–7.40 (d, J = 8 Hz, 4H), 7.04–7.02 (d, J = 8 Hz, 4H), 4.12–4.09 (t, J = 8 Hz, 4H), 2.68–2.64 (t, J = 8 Hz, 4H), 2.58–2.54 (t, J = 8 Hz, 4H), 2.05–1.98 (m, 4H), 1.65–1.59 (m, 4H) 1.30–1.23 (m, 12H), 0.84–0.81 (t, J = 8 Hz, 6H). ^{13}C NMR (100 MHz, DMSO-D_6), δ (ppm): 162.78, 158.87, 152.13, 139.77, 139.03, 136.12, 130.43, 126.26, 125.07, 115.30, 69.60, 67.28, 48.35, 31.45, 30.73, 29.02, 25.75, 22.52, 14.42. HRMS (ESI) m/z: $[M - 2Na]^{2-}$ calculated value for $C_{44}H_{50}N_2O_8S_5^{2-}$, 447.1086; found, 447.0802.

Result and discussion

The synthetic routes and chemical structure of sodium 3,3′-(((5,5′-(benzo[*c*][1,2,5]thiadiazole-4,7-diyl)bis(3-hexylthiophene-5,2-diyl))bis(4,1-phenylene))bis(oxy))bis (propane-1-sulfonate) (**TBT-a**) were shown in Scheme 1. The anionic compound **TBT-a** was synthesized by nucleophilic substitution reaction of the neutral precursor with 1,3-propane sultone in the presence of sodium hydride. The phenolic precursor **3** was simply synthesized *via* Pd(0)-catalyzed Suzuki coupling. **TBT-a** was purified by re-crystallization with alcohol/H_2O. The anionic compound **TBT-a** was not soluble in non-polar solvents, but was easily soluble in water and partially soluble in methanol, DMF and DMSO.

The UV-vis spectra of **TBT-a** aqueous solution and thin film were shown in Fig. 1a. The film was prepared by spin-coating **TBT-a** aqueous solution onto quartz substrate. In solution, the absorption maximum (λ_{abs}^{max}) of **TBT-a** was located at 338 nm and 500 nm, while the absorption maximum of film was located at 329 nm and 519 nm. The absorption in ultraviolet range was attributed to π–π* transition and the other in visible range was attributed to the intramolecular charge transfer. Compared to the absorption in solution, the absorption of **TBT-a** in film

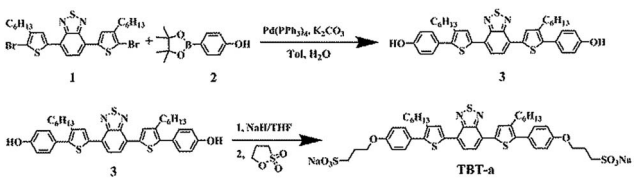

Scheme 1 Synthetic routes and chemical structure of **TBT-a**.

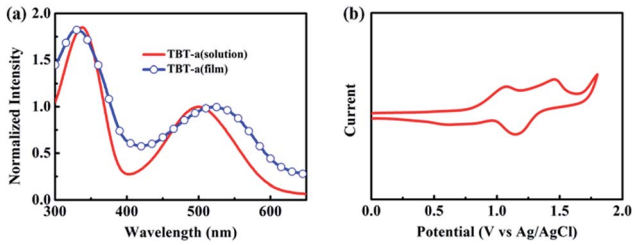

Fig. 1 (a) Normalized UV-vis absorption spectra of **TBT-a** solution and film, (b) cyclic voltammogram of **TBT-a** film in a THF solution of 0.1 mol L^{-1} Bu_4NPF_6 at a scan rate of 50 mV s^{-1}.

exhibited a bathochromic shift (about 20 nm), indicating enhanced inter-molecular interactions in the solid state.[41]

The cyclic voltammogram of **TBT-a** was shown in Fig. 1b. Energy levels were estimated by using ferrocene (Fc) ionization potential value (4.80 eV) as the standard. The highest occupied molecular orbital (HOMO) level of **TBT-a** was obtained from oxidation peak through calculation, which was −5.17 eV. According to the onset absorption, the optical band gap (E_g^{opt}) of **TBT-a** was 2.02 eV. The lowest unoccupied molecular orbital (LUMO) level of **TBT-a** was calculated from the HOMO level and E_g^{opt}, which was −3.15 eV.

In order to investigate the photovoltaic performance of the novel small molecule, we designed a conventional device configuration. The device configuration and the molecular structures of active-layer materials were shown in Fig. 2. In this structure, we used a PTB7 : $PC_{71}BM$ blend as the active-layer with an ITO/PEDOT : PSS/PTB7 : $PC_{71}BM$/interlayer/Al device configuration. The interlayer was spin-coated onto the active-layer and the optimized concentration of **TBT-a** was confirmed to be 1.0 mg mL^{-1}. As the solvent of interlayer could influence the device performance, device with active-layer treated by MeOH was also prepared as control device.[42]

Fig. 2c and d showed the current density–voltage (J–V) characteristics of the devices under light and dark conditions.

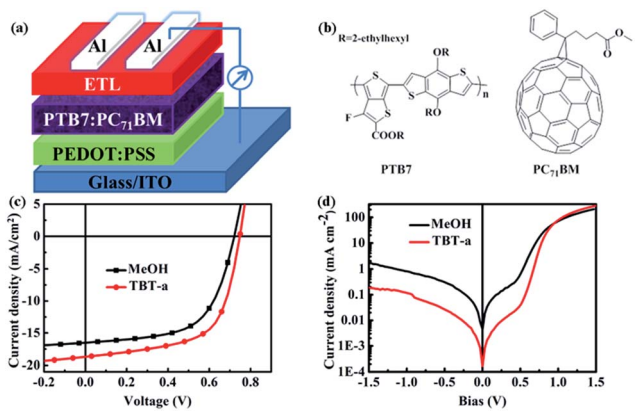

Fig. 2 (a) Conventional device structure of ITO/PEDOT : PSS/PTB7 : $PC_{71}BM$/interlayer/Al, (b) molecular structures of active-layer materials, (c) J–V characteristics of the conventional devices with MeOH treatment or **TBT-a** interlayer under 1000 W m^{-2} AM 1.5G illumination or (d) under dark conditions.

Table 1 Photovoltaic performances of PSCs based on different cathode interlayers (**TBT-a** and MeOH) under AM 1.5G irradiation (1000 W m^{-2})

Interlayer	V_{oc} (V)	J_{sc} (mA cm^{-2})	FF (%)	PCE (%)	R_s (Ω cm^2)	R_{sh} (Ω cm^2)
MeOH	0.72	16.49	60.25	7.16 (7.10)[a]	6.64	445.09
TBT-a	0.75	18.69	62.07	8.68 (8.54)[a]	5.68	300.22

[a] The average PCEs were based on 6 individual devices.

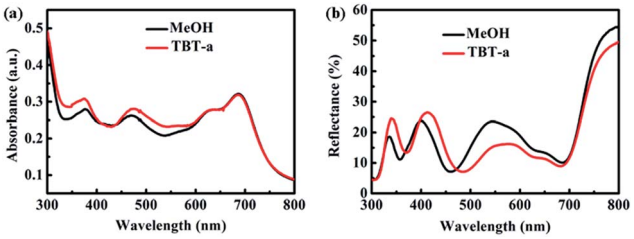

Fig. 4 (a) The absorption of ITO/PEDOT : PSS/PTB7 : $PC_{71}BM$ films with MeOH treatment or **TBT-a** interlayer, (b) the reflectance of devices with MeOH treatment or **TBT-a** interlayer.

Table 1 summarized the corresponding J_{sc}, V_{oc}, FF and PCE values. The control device presented a best PCE of 7.10%, with a J_{sc} of 16.49 mA cm^{-2}, a V_{oc} of 0.72 V, and a FF of 60.25%. Compared to the control device, the device with **TBT-a** as cathode interlayer exhibited a higher PCE of 8.68%, with a J_{sc} of 18.69 mA cm^{-2}, a V_{oc} of 0.75 V, and a FF of 62.07%. It is obvious that the insertion of **TBT-a** as cathode interlayer simultaneously increased the J_{sc}, V_{oc}, and FF. The dark *J–V* curves of the control device and **TBT-a** device were shown in Fig. 2d. In dark condition, the device with **TBT-a** as cathode interlayer exhibited a lower leakage and higher forward bias current, indicating better charge selectivity over device with MeOH treatment.[42]

It is believed that the interface dipole formed by cathode interlayer was essential to the improvement of PSC efficiency. To visualize the interfacial dipole upon the deposition of **TBT-a** interlayer, the surface potentials of active film with MeOH treatment and **TBT-a** interlayer were probed by scanning Kelvin probe microscopy (SKPM) measurements.[43–45] As shown in Fig. 3, the potential of PTB7 : $PC_{71}BM$ film with **TBT-a** interlayer was 427 mV, which was about 50 mV more positive than that of PTB7 : $PC_{71}BM$ film treated by MeOH. Since the surface potential was an extremely sensitive indicator of surface including surface reconstruction and chemical composition,[43] the 50 mV positive shifts of the surface potential upon the deposition of **TBT-a** indicated that anionic **TBT-a** induced a microscopic electric dipole moment.[45] The direction of this dipole moment was aligned with the built-in potential, which was identical to that induced by amino-based interfacial materials. Thus, the incorporation of **TBT-a** exerted an additional electrical field at the interface between active layer and Al cathode, resulting in an increasement of V_{oc}.[44]

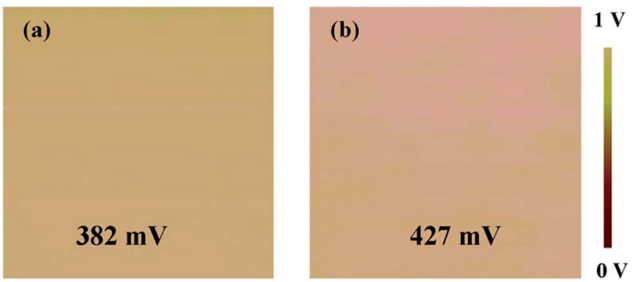

Fig. 3 Surface potential images of the PTB7 : $PC_{71}BM$ film (a) treated by MeOH and (b) with **TBT-a** interlayer (size: 2.5 μm × 2.5 μm).

In order to investigate the improvement of the J_{sc}, we got the UV-vis absorption of the ITO/PEDOT : PSS/PTB7 : $PC_{71}BM$/interlayer and reflectance spectra of MeOH treatment device and **TBT-a** device, which were shown in Fig. 4. Compared to the active-layer with MeOH treatment, PTB7 : $PC_{71}BM$/**TBT-a** exhibited a more intense absorption over 300 nm to 400 nm and 450 nm to 600 nm, which was consistent with the absorption of **TBT-a**. Thus the more intense absorption of PTB7 : $PC_{71}BM$/**TBT-a** was ascribed to the absorption of cathode interlayer, which would not induce a higher J_{sc} of the **TBT-a** device. However, it was noteworthy that the reflectance intensity in the range of 500–700 nm of **TBT-a** device was prominent weaker than that of MeOH treatment device. Although **TBT-a** exhibited an absorption band from 500 nm to 600 nm, which maybe induced a weaker reflectance of **TBT-a** device and was not benefit to the enhancement of J_{sc}, the weaker reflectance intensity from 600 nm to 700 nm should be induced by the optical interference of **TBT-a** interlayer. In this regard, the **TBT-a** interlayer played a role of optical spacer and thus increased the number of carriers per incident photon collected at the electrode.[46] Hence, the optical spacer of **TBT-a** interlayer was responsible for higher J_{sc} value of **TBT-a** device.

Atomic force microscopy (AFM) was then carried out to examine the morphologies of the photoactive layers with MeOH treatment and **TBT-a** interlayer (Fig. S6†). We found that the surface of PTB7 : $PC_{71}BM$/**TBT-a** was rougher than that of PTB7 : $PC_{71}BM$ film, which could induce a different interfacial adhesion and electron transporting and extraction.[47] To investigate the electron transport properties of the device with and without interlayers, electron-only devices with the configuration of ITO/Al/PTB7 : $PC_{71}BM$/MeOH treatment or **TBT-a**/Al were prepared and characterized. *J–V* curves for the interlayers of electron-only devices were appeared in Fig. 5a. Current density of **TBT-a** device was obviously higher than MeOH treatment device. The electron mobility of the device was deduced by fitting the *J–V* curves with the Mott–Gurney law.[44,48] As shown in Fig. 5b, the electron mobility was determined to be 2.53×10^{-5} $cm^2\ V^{-1}\ s^{-1}$ for **TBT-a** device, which was 5 times higher than the MeOH treatment device. This enhanced electron mobility indicated that **TBT-a** was benefit for electron collecting and transporting and could also lead to a high J_{sc}. The combination of higher electron mobility combination and electrical field modulation of **TBT-a** was deduced to the high J_{sc} of **TBT-a** device.

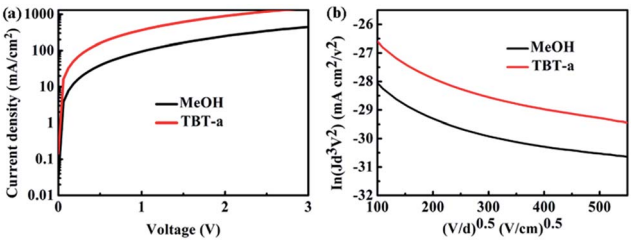

Fig. 5 (a) Measured *J*–*V* curves for electron-only devices. Results were obtained using the space charge limited current (SCLC) method for ITO/Al (200 nm)/PTB7 : $PC_{71}BM$ (100 nm)/interlayer/Al (200 nm) structures, (b) $\ln(Jd^3/V^2)$ *versus* $(V/d)^{0.5}$ plots of ITO/Al/PTB7 : $PC_{71}BM$ (100 nm)/interlayer/Al for the measurement of electron mobility by the SCLC method.

Conclusions

In conclusion, a novel non-amino small molecule based on sulfonate anion was designed and synthesized as a cathode interfacial material for conventional PSC. Compared to the device without cathode interlayer, the device with **TBT-a** as cathode interlayer exhibited an enhancement in both V_{oc}, J_{sc} and FF, with a highest PCE value of 8.68%. Similar to the amino-based cathode interfacial materials, **TBT-a** could effectively reduce the work function of cathode, play a role as optical spacer, and enhance the electron mobility of the device. According to the literature, conjugated polyelectrolytes with sulfonate anion were usually used as anode interfacial materials. However, our results indicate that sulfonate derivatives could also be candidates for cathode interfacial materials of PSCs, which will broaden the material types of cathode interfacial materials and be helpful for the research on the effect of ions in interface modification.

Acknowledgements

This research was supported by National Natural Science Foundation of China (No. 51273208, 61474125, 51403222), Zhejiang Provincial Natural Science Foundation of China (LR14E030002), and Ningbo Science and Technology Bureau (2014B82010). The work was also supported by National Young Top-Notch Talent Program of China and Hundred Talent Program of Chinese Academy of Sciences.

Notes and references

1 H.-Y. Chen, J. Hou, S. Zhang, Y. Liang, G. Yang, Y. Yang, L. Yu, Y. Wu and G. Li, *Nat. Photonics*, 2009, **3**, 649–653.
2 J. Zhou, X. Wan, Y. Liu, Y. Zuo, Z. Li, G. He, G. Long, W. Ni, C. Li, X. Su and Y. Chen, *J. Am. Chem. Soc.*, 2012, **134**, 16345–16351.
3 G. H. Jun, S. H. Jin, B. Lee, B. H. Kim, W.-S. Chae, S. H. Hong and S. Jeon, *Energy Environ. Sci.*, 2013, **6**, 3000–3006.
4 X. Guo, N. Zhou, S. J. Lou, J. Smith, D. B. Tice, J. W. Hennek, R. P. Ortiz, J. T. L. Navarrete, S. Li, J. Strzalka, L. X. Chen, R. P. H. Chang, A. Facchetti and T. J. Marks, *Nat. Photonics*, 2013, **7**, 825–833.
5 C. Duan, K. Zhang, C. Zhong, F. Huang and Y. Cao, *Chem. Soc. Rev.*, 2013, **42**, 9071–9104.
6 J. D. Chen, C. Cui, Y. Q. Li, L. Zhou, Q. D. Ou, C. Li, Y. Li and J. X. Tang, *Adv. Mater.*, 2015, **27**, 1035–1041.
7 C. Zhong, F. Huang, Y. Cao, D. Moses and A. J. Heeger, *Adv. Mater.*, 2014, **26**, 2341–2345.
8 W. Zhang, Y. Wu, Q. Bao, F. Gao and J. Fang, *Adv. Energy Mater.*, 2014, **4**, 1400359.
9 B. Meng, Z. Wang, W. Ma, Z. Xie, J. Liu and L. Wang, *Adv. Funct. Mater.*, 2016, **2**, 226–232.
10 B. Kan, Q. Zhang, M. Li, X. Wan, W. Ni, G. Long, Y. Wang, X. Yang, H. Feng and Y. Chen, *J. Am. Chem. Soc.*, 2014, **136**, 15529–15532.
11 Z. He, C. Zhong, S. Su, M. Xu, H. Wu and Y. Cao, *Nat. Photonics*, 2012, **6**, 593–597.
12 T. Aytun, L. Barreda, A. Ruiz-Carretero, J. A. Lehrman and S. I. Stupp, *Chem. Mater.*, 2015, **27**, 1201–1209.
13 Q. Zhang, D. Zhang, X. Li, X. Liu, W. Zhang, L. Han and J. Fang, *Chem. Commun.*, 2015, **51**, 10182–10185.
14 J. Zhou, Y. Zuo, X. Wan, G. Long, Q. Zhang, W. Ni, Y. Liu, Z. Li, G. He and C. Li, *J. Am. Chem. Soc.*, 2013, **135**, 8484–8487.
15 Z. Tan, D. Qian, W. Zhang, L. Li, Y. Ding, Q. Xu, F. Wang and Y. Li, *J. Mater. Chem. A*, 2013, **1**, 657–664.
16 P. Cai, H. Jia, J. Chen and Y. Cao, *ACS Appl. Mater. Interfaces*, 2015, **7**, 27871–27877.
17 K. Yao, M. Salvador, C.-C. Chueh, X.-K. Xin, Y.-X. Xu, D. W. deQuilettes, T. Hu, Y. Chen, D. S. Ginger and A. K. Y. Jen, *Adv. Energy Mater.*, 2014, **4**, 1400206.
18 S. Liu, K. Zhang, J. Lu, J. Zhang, H.-L. Yip, F. Huang and Y. Cao, *J. Am. Chem. Soc.*, 2013, **135**, 15326–15329.
19 Z. A. Page, Y. Liu, V. V. Duzhko, T. P. Russell and T. Emrick, *Science*, 2014, **346**, 441–444.
20 S.-H. Liao, Y.-L. Li, T.-H. Jen, Y.-S. Cheng and S.-A. Chen, *J. Am. Chem. Soc.*, 2012, **134**, 14271–14274.
21 Y. Zhang, L. Chen, X. Hu, L. Zhang and Y. Chen, *Sci. Rep.*, 2015, **5**, 12839.
22 H. J. Song, E. J. Lee, D. H. Kim, T. H. Lee, M. Goh, S. Lee and D. K. Moon, *Dyes Pigm.*, 2015, **113**, 210–218.
23 J.-S. Yeo, M. Kang, Y.-S. Jung, R. Kang, S.-H. Lee, Y.-J. Heo, S.-H. Jin, D.-Y. Kim and S.-I. Na, *Nano Energy*, 2016, **21**, 26–38.
24 H. J. Song, E. J. Lee, D. H. Kim, D. K. Moon and S. Lee, *Sol. Energy Mater. Sol. Cells*, 2015, **141**, 232–239.
25 X. Li, W. Zhang, X. Wang, F. Gao and J. Fang, *ACS Appl. Mater. Interfaces*, 2014, **6**, 20569–20573.
26 Y. Zhu, X. Xu, L. Zhang, J. Chen and Y. Cao, *Sol. Energy Mater. Sol. Cells*, 2012, **97**, 83–88.
27 W. Zhang, C. Min, Q. Zhang, X. Li and J. Fang, *Org. Electron.*, 2014, **15**, 3632–3638.
28 Z. Wu, C. Sun, S. Dong, X. Jiang, S. Wu, H. Wu, H. Yip, F. Huang and Y. Cao, *J. Am. Chem. Soc.*, 2016, **138**, 2004–2013.
29 J. H. Seo, A. Gutacker, Y. Sun, H. Wu, F. Huang, Y. Cao, U. Scherf, A. J. Heeger and G. C. Bazan, *J. Am. Chem. Soc.*, 2016, **133**, 8416–8419.

30 L. Hu, F. Wu, C. Li, A. Hu, X. Hu, Y. Zhang, L. Chen and Y. Chen, *Macromolecules*, 2015, **48**, 5578–5586.
31 M. Lv, S. Li, J. J. Jasieniak, J. Hou, J. Zhu, Z. A. Tan, S. E. Watkins, Y. Li and X. Chen, *Adv. Mater.*, 2013, **25**, 6889–6894.
32 Z.-G. Zhang, H. Li, B. Qi, D. Chi, Z. Jin, Z. Qi, J. Hou, Y. Li and J. Wang, *J. Mater. Chem. A*, 2013, **1**, 9624–9629.
33 C.-H. Wu, C.-Y. Chin, T.-Y. Chen, S.-N. Hsieh, C.-H. Lee, T.-F. Guo, A. K.-Y. Jen and T.-C. Wen, *J. Mater. Chem. A*, 2013, **1**, 2582–2587.
34 Y. Zhao, Z. Xie, C. Qin, Y. Qu, Y. Geng and L. Wang, *Sol. Energy Mater. Sol. Cells*, 2009, **93**, 604–608.
35 R. Kang, S.-H. Oh and D.-Y. Kim, *ACS Appl. Mater. Interfaces*, 2014, **6**, 6227–6236.
36 B. Xu, Z. Zheng, K. Zhao and J. Hou, *Adv. Mater.*, 2016, **28**, 434–439.
37 T. V. Pho, H. Kim, J. H. Seo, A. J. Heeger and F. Wudl, *Adv. Funct. Mater.*, 2011, **21**, 4338–4341.
38 F. Liu, Z. A. Page, V. V. Duzhko, T. P. Russell and T. Emrick, *Adv. Mater.*, 2013, **25**, 6868–6873.
39 T. Yasuda, Y. Shinohara, T. Matsuda, L. Han and T. Ishi-i, *J. Polym. Sci., Part A: Polym. Chem.*, 2013, **51**, 2536–2544.
40 M. J. Waring, A. M. Birch, S. Birtles, L. K. Buckett, R. J. Butlin, L. Campbell, P. M. Gutierrez, P. D. Kemmitt, A. G. Leach, P. A. MacFaul, C. O'Donnell and A. V. Turnbull, *MedChemComm*, 2013, **4**, 159–164.
41 V. Mimaite, J. Ostrauskaite, D. Gudeika, J. V. Grazulevicius and V. Jankauskas, *Synth. Met.*, 2011, **161**, 1575–1581.
42 H. Zhou, Y. Zhang, J. Seifter, S. D. Collins, C. Luo, G. C. Bazan, T. Q. Nguyen and A. J. Heeger, *Adv. Mater.*, 2013, **25**, 1646–1652.
43 L. S. C. Pingree, O. G. Reid and D. S. Ginger, *Adv. Mater.*, 2009, **21**, 19–28.
44 Z. He, C. Zhong, X. Huang, W.-Y. Wong, H. Wu, L. Chen, S. Su and Y. Cao, *Adv. Mater.*, 2011, **23**, 4636–4643.
45 W. Osikowicz, M. P. de Jong and W. R. Salaneck, *Adv. Mater.*, 2007, **19**, 4213–4217.
46 J. Liu, S. Shao, G. Fang, B. Meng, Z. Xie and L. Wang, *Adv. Mater.*, 2012, **24**, 2774–2779.
47 T. Yang, M. Wang, C. Duan, X. Hu, L. Huang, J. Peng, F. Huang and X. Gong, *Energy Environ. Sci.*, 2012, **5**, 8208.
48 M. Kiy, P. Losio, I. Biaggio, M. Koehler, A. Tapponnier and P. Günter, *Appl. Phys. Lett.*, 2002, **80**, 1198.